NANOSYSTEMS: PHYSICS, CHEMISTRY, MATHEMATICS, 2015, 6 (5), P. 715–725

# Cryometry and excess functions of the adduct of light fullerene $C_{60}$ and arginine – $C_{60}(C_6H_{12}NaN_4O_2)_8H_8$ aqueous solutions

M. Yu. Matuzenko[1], A. A. Shestopalova[1], K. N. Semenov[2], N. A. Charykov[3,1], V. A. Keskinov[1]

[1]St. Petersburg State Technological Institute (Technical University), St. Petersburg, Russia
[2]St. Petersburg State University, St. Petersburg, Russia
[3]St. Petersburg State Electro-technical University (LETI), St. Petersburg, Russia
keskinov@mail.ru

**PACS 61.48.+c** **DOI 10.17586/2220-8054-2015-6-5-715-725**

Cryometry investigation of $C_{60}(C_6H_{12}NaN_4O_2)_8H_8$ - $H_2O$ solutions was made over concentrations ranging from 0.1 – 10 g of fullerene-arginine adduct per 1 $dm^3$. Freezing point depression was measured for these aqueous solutions. Excess functions for water and fullerene-arginine adduct activities, activity coefficients and excess Gibbs energy of the solutions were calculated. All solutions demonstrate huge deviations from ideality. The last fact, to our opinion, is caused by the very specific – hierarchical type of association of fullerene-arginine adducts in aqueous solution components, which is proved by the results of our visible light scattering analysis.

**Keywords:** cryometry, activities, activity coefficients, fullerene-arginine adduct, water solution.

*Received: 11 April 2015*

*Revised: 15 April 2015*

## 1. Introduction

This article is a continuation in the series of articles devoted to the synthesis, identification and physico-chemical properties investigation of nanoclusters, which represented the fairly water soluble derivatives of light fullerenes $C_{60}$ and $C_{70}$ [1–14] – poly-hydroxylated fullerenols $\left(\text{fullerenol-d } C_{60}(OH)_{24\pm2}\right.$ and malonic ether – trismalonate $\left.C_{70}[=C(COOH)_2]_3\right)$. In previous articles, the authors have reported on the volume, refraction, electrical, transport properties of water soluble nanoclusters and their aqueous solutions. Also, the investigations of solubility in water under poly-thermal conditions as well as in some ternary water-salt systems and complex thermal analysis of nanocluster crystal-hydrates were made.

## 2. The synthesis of the adduct of light fullerene $C_{60}$ with arginine $C_{60}(C_6H_{13}N_4O_2)_8H_8$

Arginine hydrochloride ($L–C_6H_{14}N_4O_2{\cdot}HCl$) (5 g) and sodium hydroxide (2.5 g) were dissolved in 30 ml of water and 200 ml $CH_3CH_2OH$. In the other vessel fullerene $C_{60}$ (0.5 g) was dissolved in 80 ml $o–C_6H_4(CH_3)_2$. Then both solutions were combined, mixed and remained at room temperature for 120 hours. A deep-brown exfoliating solution was formed. The colorless organic phase was separated from the aqueous inorganic one. The aqueous phase was salted using excess methanol ($CH_3OH$) over 24 hours. At that time, the sedimentation of the of the light fullerene $C_{60}$ adduct with arginine was completed. The precipitate was filtered and washed repeatedly with a mix of $CH_3OH$ with concentrated HCl. Recrystallization of precipitate was performed 3 times. Finally, the precipitate was dried at 60 °C for 8 hours. Previously, the synthesis of an original $\beta$-alanine $C_{60}$ adduct was described [18]. Correspondingly, the L-arginine – light fullerene $C_{60}$ adduct was formed – $C_{60}(C_6H_{12}NaN_4O_2)_8H_8$ with a yield $\approx$ 80 %.

## 3. Reasons for direct excess functions in fullerene-arginine adduct – water solutions determination

The authors do not know of any direct experimental data concerning the determination of the excess thermodynamic data (primarily activity coefficients) in binary (or more component) solutions of fullerenes or their derivatives in any solutions. This fact may, to our opinion, be explained by the very low solubility of such nanoclusters in the majority of solvents (see, for example [15–17]). For fairly water soluble nanoclusters (e.g.: poly-hydroxylated fullerenols $C_{60}(OH)_n$, $C_{70}(OH)_n$; some esters – for example: trismalonic esters – trismalonate $C_{60}[=C(COOH)_2]_3$, $C_{70}[=C(COOH)_2]_3$, some adducts with amino-acids (for example arginine $C_{60}(C_6H_{12}NaN_4O_2)_8H_8$ or alanine [18]), their solubility in water, which depends on the type of nanocluster and temperature, may vary from tens to hundreds grams of nanocluster per $dm^3$ of solvent. This fact permitted us to determine excess functions of the solution by standard methods, for example, cryometry (as described in the present article) or by the determination of water activity by isopiestic method. Such determination is, to our opinion, may be very interesting because of the following reasons.

Visible light scattering analysis in $C_{60}(C_6H_{12}NaN_4O_2)_8H_8$ – water solutions (as well as in light fullerenols (trismalonates)-water solutions) at room temperature was provided repeatedly (see [1, 5, 14]). In all cases, one can observe the following:

- No monomer molecular nanoclusters (with linear dimension diameter $d_0 \approx 1.5$ – 2.0 nm) are seen in all investigated solutions, even in the dilute solution ($C = 0.1$ g/dm$^3$).
- The diameters of the first type aggregates (the first order clusters of percolation) have the similar order – tens of nm $d_1 \approx 20$ – 80 nm over the entire concentration range.
- The diameters of the second type aggregates (the second order clusters of percolation) also have a similar order – hundreds nm $d_2 \approx 100$ – 400 nm.
- The third type associates (the third order clusters of percolation) have not been seen at any concentrations except in the most highly concentrated solution at $C > 1$ g/dm$^3$, where clusters with extremely huge linear dimension (on the order of microns) are formed: $d_3 > 1000$ nm – the solution 'becomes very heterogeneous' but stable as a colloidal system.
- Thus, to describe such facts in the aggregation process, a stepwise model of particle growth was invoked, in other words, a hierarchical type of association of fullerenols (trismalonates) components was observed in aqueous solutions. We consider that monomer spherical molecules form the first type of spherical aggregates, then, the first type spherical associates form a second type of spherical associates. Next, the second type of spherical associates form a third type spherical associates (the last ones correspond to a heterogeneous colloidal system). A typical figure of the distribution for $C_{60}(C_6H_{12}NaN_4O_2)_8H_8$ nanoclusters in aqueous solutions at comparatively high concentrations is represented below – in Fig. 1 (the third type associates).

## 4. The possibility of the determination of the excess functions in $C_{60}(C_6H_{12}NaN_4O_2)_8H_8$ – water solutions

In order to check the possibility of determining the excess functions in $C_{60}(C_6H_{12}NaN_4O_2)_8H_8$ – $H_2O$ solutions in the selected concentration range by cryometry method one must be sure of the following:

- Solubility in the binary system $C_{60}(C_6H_{12}NaN_4O_2)_8H_8$ – $H_2O$ at a temperature of 273.15 K is great enough such that the solution is formally homogeneous, i.e. does not consist of solid $C_{60}(C_6H_{12}NaN_4O_2)_8H_8$ crystal hydrates. Preliminary experiments show

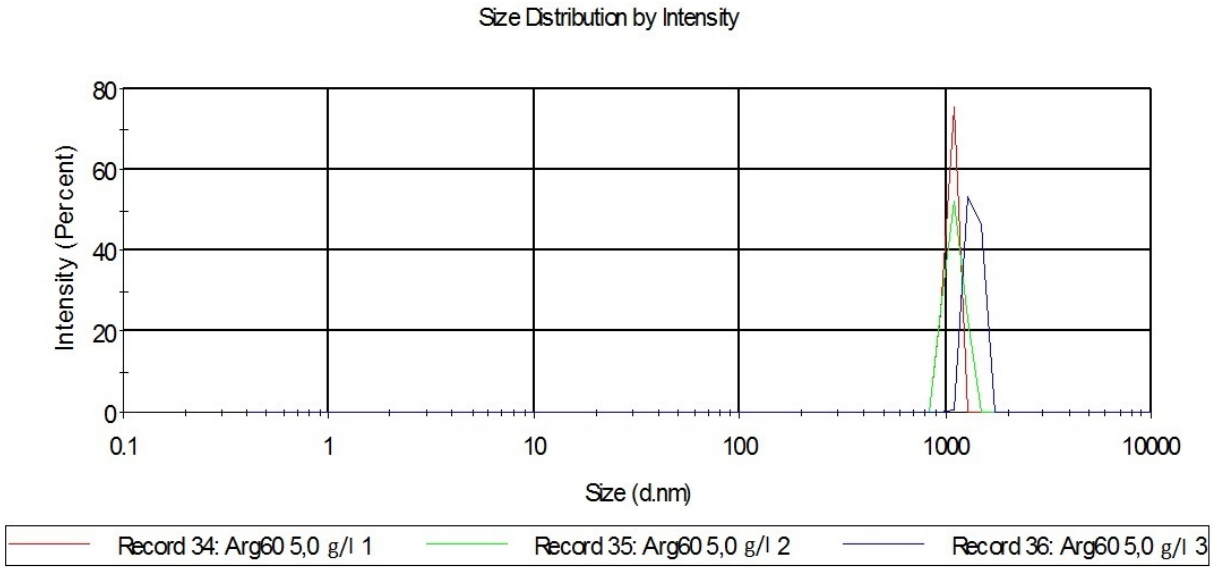


FIG. 1. The linear dimension of the particles on the base of the adducts $C_{60}(C_6H_{12}NaN_4O_2)_8H_8$ in aqueous ($\delta$) solutions at $C = 5$ g/dm$^3$ (different curves correspond to the different times of observation (signal integration)

that in both cases, the solubility of $C_{60}(C_6H_{12}NaN_4O_2)_8H_8$ nanoclusters at 273.15±1 K is $\approx 70$ g/dm$^3$. So, if we set the concentration range at not more than tens g/dm$^3$, we can be sure that no solid crystal hydrates can co-crystallize with water ice during the crystallization.

– Additionally, one must be sure that the nanocluster solutions are really homogeneous – do not delaminate and are not colloidal. In our case, only more or less diluted solutions may satisfy these request (see lower).
– The last condition is that the temperature decrease $\Delta T$ should be more or less significant – hundredths, or even better tenth of a degree K. Fortuitously, this request is easily satisfied.

## 5. Cryometry investigation in the binary system: $C_{60}(C_6H_{12}NaN_4O_2)_8H_8$ – $H_2O$. The decrease of the temperatures of the beginning of the $H_2O$ – ice crystallization in $C_{60}(C_6H_{12}NaN_4O_2)_8H_8$ – water solutions. Cryometry of water solutions of water soluble fullerene derivatives. Main thermodynamic equations

Let us introduce designation:

$$\Delta F = F^S - F^L, \quad \Delta T = T_0^f - T, \tag{1}$$

where $T_0^f$ – melting point of pure solvent, for water $T_0^f = 273.15$ K, $T$ – current temperature (K), $\Delta F$ – molar change of thermodynamic function $F$, $F^S$ – molar function $F$ for the solid phase, $F^L$ – molar function $F$ for the liquid phase.

The conditions for chemical phase equilibrium liquid ($L$) – solid ($S$) for the pure solvent – water ($W$) were as follows:

$$\mu w_0^S = \mu w_0^L + RT \ln a_W \tag{2}$$

where: $\mu w_0^S$, $\mu w_0^L$ – standard chemical potential of the solvent – water, in the solid and liquid phases, correspondingly, $a_W$ – water activity in the scale of molar fractions in symmetrical normalization scale. Thus:

$$-\Delta H_W^f + \Delta C_P \left(T - T_0^f\right) + T\left[\Delta S_W^f - \Delta C_P \ln\left(T/T_0^f\right)\right] = RT \ln a_W, \tag{3}$$

$$\ln\left(T/T_0^f\right) = \ln\left(T_0^f - \Delta T/T_0^f\right) = \ln\left(1 - \Delta T/T_0^f\right) \approx -\Delta T/T_0^f, \tag{4}$$

where: $\Delta H_W^f$, $\Delta S_W^f$, $\Delta C_P$ – molar enthalpy, entropy and change of isobaric heat capacity of water at the temperature $T_0^f$. So:

$$-\Delta H_W^f \left[1 - T/T_0^f\right] + \Delta C_P \left[T - T_0^f - T \ln\left(T/T_0^f\right)\right] = RT \ln a_W, \tag{5.1}$$

$$-\Delta H_W^f \Delta T/T_0^f + \Delta C_P \Delta T \left(-1 + T/T_0^f\right) = RT \ln a_W, \tag{5.2}$$

$$\frac{-\Delta H_W^f \Delta T - \Delta C_P \Delta T^2}{R\left(T_0^f - \Delta T\right) T_0^f} = \ln a_W. \tag{5.3}$$

Later, we shall use formula (5.3) as the basis for calculating the excess solution functions. In all calculations, we will use symmetrical normalization of the excess functions, as if nanoclusters are very weak electrolytes – practically non-electrolytic (see nanocluster-water systems close to our system, for example [4, 6, 12]). Accordingly, we assume that:

$$a_{\mathrm{H2O}}(\mathrm{x}_{\mathrm{H2O}} = 1) = \gamma_{\mathrm{H2O}}(\mathrm{x}_{\mathrm{H2O}} = 1) = 1, \tag{6.1}$$

$$a_{\mathrm{nanocluster}}(\mathrm{x}_{\mathrm{nanocluster}} = 1) = \gamma_{\mathrm{nanocluster}}(\mathrm{x}_{\mathrm{nanocluster}} = 1) = 1, \tag{6.2}$$

where: $a_i$, $\gamma_i$ – activity and activity coefficients of $i$-th solution component.

Experimental data were obtained with the help of metastatic Beckman thermometer. Data are represented in the Fig. 2 and Table 1. Arrow in the Fig. 2 shows the temperature decrease in the case of an ideal non-electrolyte solution. Thus, one can see the huge temperature decrease we observed for our water soluble nanoclusters solutions.

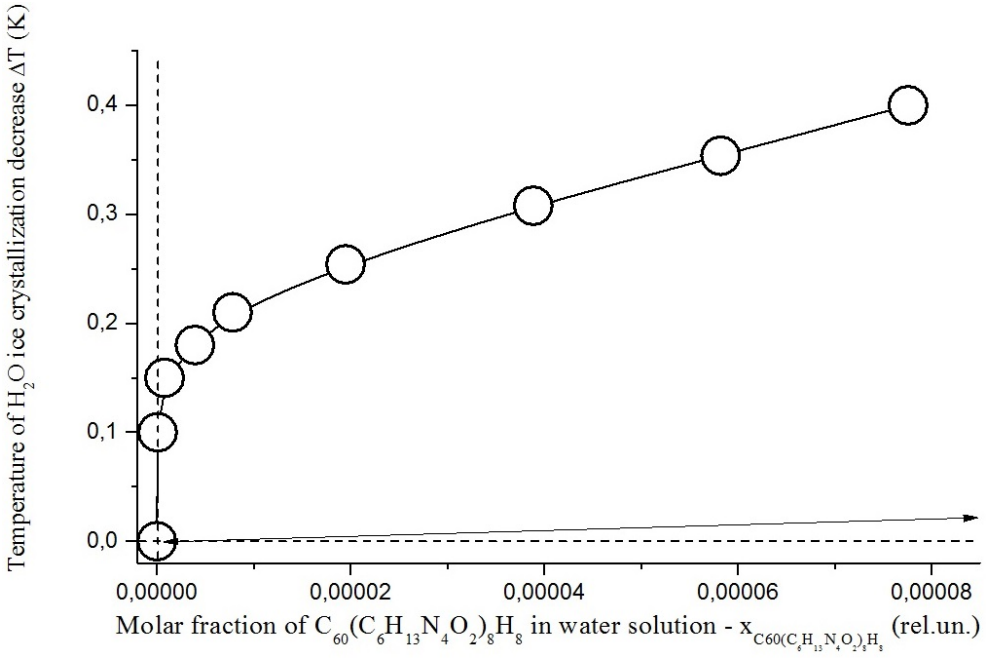


FIG. 2. The decrease of the temperatures of the beginning of the $H_2O$ – ice crystallization in $C_{60}(C_6H_{12}NaN_4O_2)_8H_8$ – water solutions ($\Delta T = 273.15 - T$)

TABLE 1. Cryometry data and excess function in the binary $C_{60}(C_6H_{12}NaN_4O_2)_8H_8$ – $H_2O$ solutions at 273.15 K

| Number | Molar fraction of $C_{60}(C_6H_{13}N_4O_2)_8H_8$ in solution $x_{C60(C6H13N4O2)8H8}$ (rel.un.) | Temperature of water crystallization decrease $\Delta T$ (K) | $\ln a_{H2O}$ (water activity) (rel.un.) | $a_{H2O}$ (water activity) (rel.un.) |
|---|---|---|---|---|
| 1 | 0.000 | 0.000 | 0.000 | 1.00000 |
| 2 | $7.868 \cdot 10^{-8}$ | 0.099 | $-9.561 \cdot 10^{-4}$ | 0.99904 |
| 3 | $7.868 \cdot 10^{-7}$ | 0.151 | −0.00146 | 0.99854 |
| 4 | $3.923 \cdot 10^{-6}$ | 0.179 | −0.00172 | 0.99827 |
| 5 | $7.828 \cdot 10^{-6}$ | 0.210 | −0.00202 | 0.99797 |
| 6 | $1.949 \cdot 10^{-5}$ | 0.254 | −0.00245 | 0.99755 |
| 7 | $3.887 \cdot 10^{-5}$ | 0.308 | −0.00297 | 0.99703 |
| 8 | $5.821 \cdot 10^{-5}$ | 0.354 | −0.00341 | 0.99658 |
| 9 | $7.758 \cdot 10^{-5}$ | 0.401 | −0.00387 | 0.99613 |

| Number | $\ln \gamma_{H2O}$ (water activity coefficient) (rel.un.) | derivative $\frac{d \ln \gamma_{H2O}}{dx_{C60(C6H13N4O2)8H8}}$ (rel.un.) | derivative $\frac{d \ln \gamma_{C60(C6H13N4O2)8H8}}{dx_{C60(C6H13N4O2)8H8}}$ (rel.un.) | $\ln \gamma_{C60(C6H13N4O2)8H8}$ (rel.un.) |
|---|---|---|---|---|
| 1 | 0.000 | −12000 | $4.2 \cdot 10^{10}$ | |
| 2 | $-9.561 \cdot 10^{-4}$ | −6300 | $1.3 \cdot 10^{10}$ | $9.2 \cdot 10^{6}$ |
| 3 | −0.00146 | −410 | $5.2 \cdot 10^{8}$ | 3750 |
| 4 | −0.00172 | −81 | $2.1 \cdot 10^{7}$ | 4100 |
| 5 | −0.00202 | −55 | $7.0 \cdot 10^{6}$ | 4130 |
| 6 | −0.00243 | −31 | $1.6 \cdot 10^{6}$ | 4150 |
| 7 | −0.00293 | −24 | $6.2 \cdot 10^{5}$ | 4170 |
| 8 | −0.00336 | −22 | $3.8 \cdot 10^{5}$ | 4180 |
| 9 | −0.00379 | −22 | $2.8 \cdot 10^{5}$ | 4200 |

| Number | $\ln a_{C60(C6H13N4O2)8H8}$ (rel.un.) | $G^{ex}/RT$ (rel.un.) | $G^{mix}/RT$ (rel.un.) | |
|---|---|---|---|---|
| 1 | 0.00000 | 0.00000 | 0.00000 | |
| 2 | $9.2 \cdot 10^{6}$ | −8.83 | −8.83 | |
| 3 | 3740 | 0.00149 | 0.00148 | |
| 4 | 4090 | 0.0143 | 0.0143 | |
| 5 | 4120 | 0.0303 | 0.0302 | |
| 6 | 4140 | 0.0784 | 0.0782 | |
| 7 | 4160 | 0.159 | 0.158 | |
| 8 | 4170 | 0.239 | 0.239 | |
| 9 | 4190 | 0.322 | 0.321 | |

## 6. Excess partial functions of water $C_{60}(C_6H_{12}NaN_4O_2)_8H_8$ components in the binary system: $C_{60}(C_6H_{12}NaN_4O_2)_8H_8$ – $H_2O$

The graph of the dependence ln of water activity ($\ln a_{H2O}$), ln of water activity coefficient ($\ln \gamma_{H2O}$), against the molar fraction of $C_{60}(C_6H_{12}NaN_4O_2)_8H_8$ in aqueous solutions are represented in Figs. 3, 4 and in Table 1. The dependence of the derivative of ln of water (nanocluster) activity coefficients ($d \ln \gamma_{H2O}/dx_{nanocluster}$) and ($d \ln \gamma_{nanocluster}/dx_{nanocluster}$) in $C_{60}(C_6H_{12}NaN_4O_2)_8H_8$ – water solutions against the molar fraction of $C_{60}(C_6H_{12}NaN_4O_2)_8H_8$ in aqueous solutions are also represented in Figs. 5, 6 (curves – approximation, points – experimental data). The approximation is represented in the Figs. 5, 6 also. For calculation, we have used the Gibbs-Duheim equation:

$$\left(\frac{\partial \ln a_{\text{nanocluster}}}{\partial \ln x_{\text{nanocluster}}}\right)_T = -\frac{x_{H2O}}{x_{\text{nanocluster}}}\left(\frac{\partial \ln a_{H2O}}{\partial \ln x_{H2O}}\right)_T. \tag{7}$$

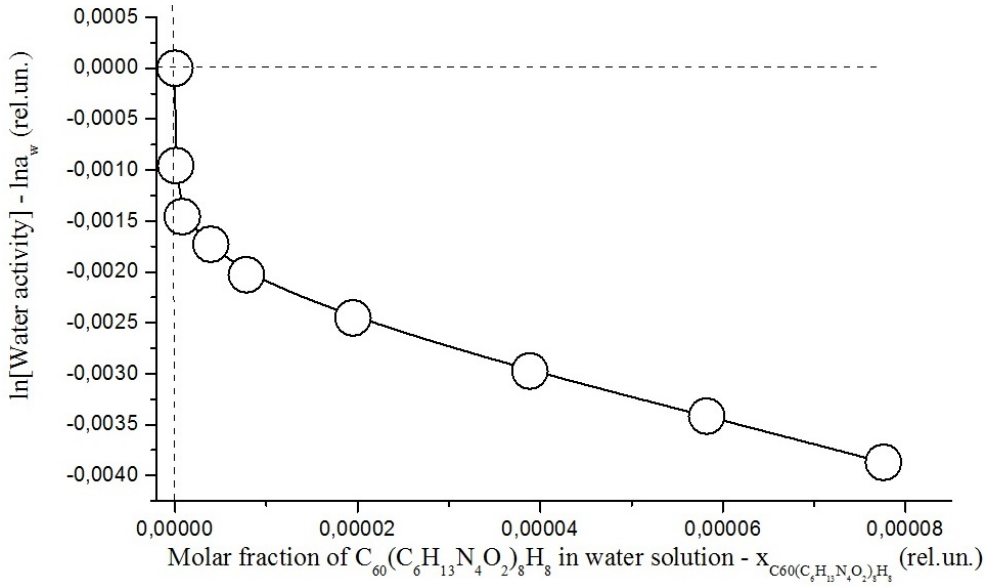


FIG. 3. The dependence of ln of water activity ($\ln a_{H2O}$) in $C_{60}(C_6H_{12}NaN_4O_2)_8H_8$ – water solutions against the molar fraction of $C_{60}(C_6H_{12}NaN_4O_2)_8H_8$ in aqueous solutions

The dependence of the ln of $C_{60}(C_6H_{12}NaN_4O_2)_8H_8$ activity coefficients ($\ln \gamma_{\text{nanocluster}}$) and ln of $C_{60}(C_6H_{12}NaN_4O_2)_8H_8$ activity ($\ln a_{\text{nanocluster}}$) in $C_{60}(C_6H_{12}NaN_4O_2)_8H_8$ – water solutions against the molar fraction of $C_{60}(C_6H_{12}NaN_4O_2)_8H_8$ in aqueous solutions are represented in Figs. 7, 8 and Table 1.

## 7. Excess and Mixing Gibbs energy in the binary system: $C_{60}(C_6H_{12}NaN_4O_2)_8H_8$ – $H_2O$. Miscibility gap and micro-heterogeneous behavior of the solutions

We have also calculated the dependence of the excess Gibbs energy of the solutions ($G^{ex}$) in $C_{60}(C_6H_{12}NaN_4O_2)_8H_8$ – water solutions against the logarithm of the $C_{60}(C_6H_{12}NaN_4O_2)_8H_8$ molar fraction in aqueous solutions (Fig. 9) and the dependence of the Gibbs energy mixing for solutions ($G^{mix}$) and the miscibility gap in $C_{60}(C_6H_{12}NaN_4O_2)_8H_8$ – water solutions against the logarithm of the $C_{60}(C_6H_{12}NaN_4O_2)_8H_8$ molar fraction (Fig. 10) and also Table 1:

$$G^{ex} = RT\left[\ln \gamma_{\text{nanocluster}} + x_{H2O} \ln \gamma_{H2O}\right], \tag{8}$$

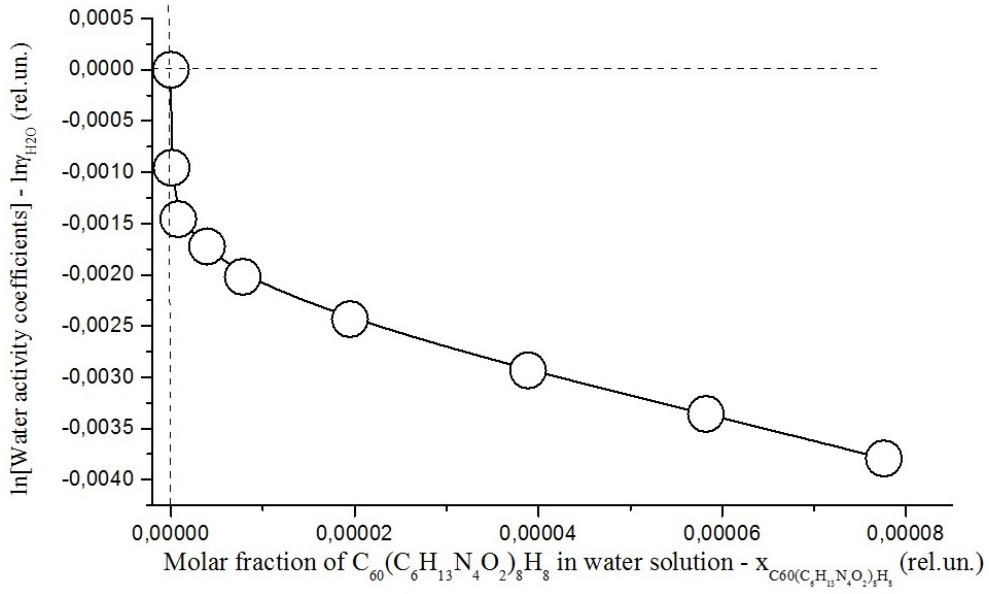


FIG. 4. The dependence of ln of water activity coefficients ($\ln \gamma_{H2O}$) in $C_{60}(C_6H_{12}NaN_4O_2)_8H_8$ – water solutions against the molar fraction of $C_{60}(C_6H_{12}NaN_4O_2)_8H_8$) in aqueous solutions

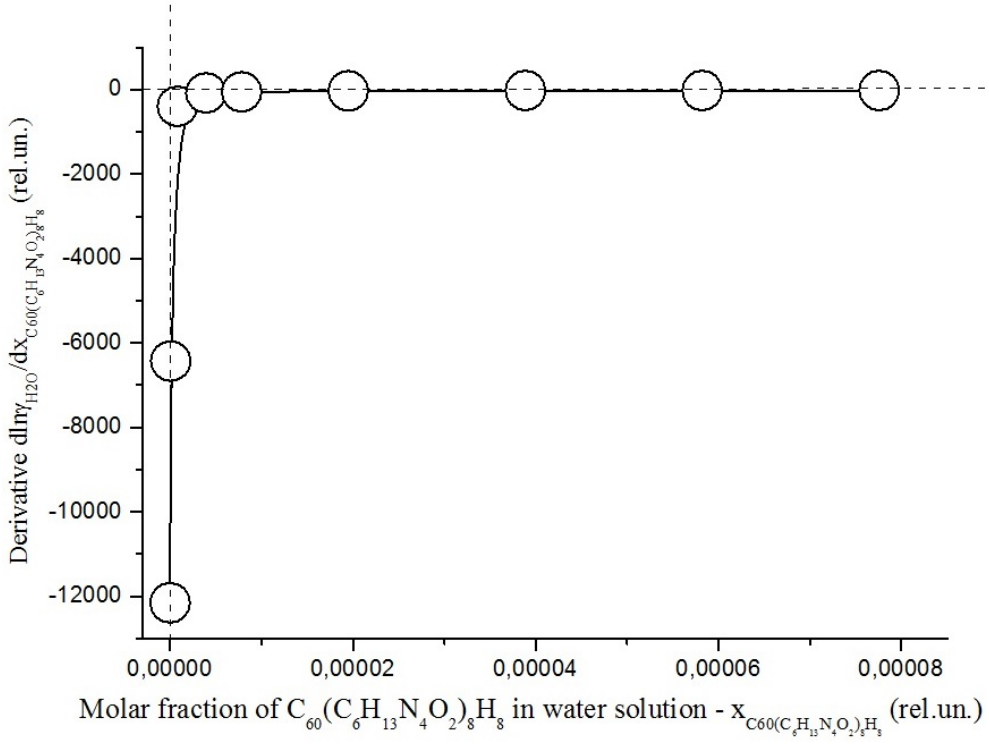


FIG. 5. The dependence of the derivative of ln of water activity coefficients ($d \ln \gamma_{H2O}/dx_{nanocluster}$) in $C_{60}(C_6H_{12}NaN_4O_2)_8H_8$ – water solutions against the molar fraction of $C_{60}(C_6H_{12}NaN_4O_2)_8H_8$ in aqueous solutions (curves – approximation, points – experimental data)

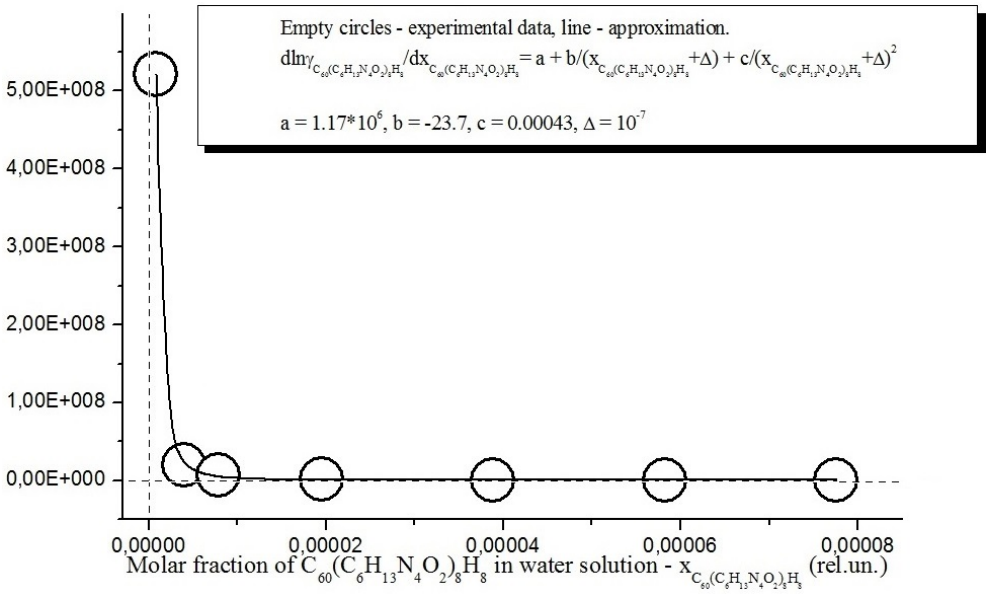


FIG. 6. The dependence of the derivative of ln of $C_{60}(C_6H_{12}NaN_4O_2)_8H_8$ activity coefficients ($d\ln\gamma_{\text{nanocluster}}/dx_{\text{nanocluster}}$) in $C_{60}(C_6H_{12}NaN_4O_2)_8H_8$ – water solutions against the molar fraction of $C_{60}(C_6H_{12}NaN_4O_2)_8H_8$ in aqueous solutions

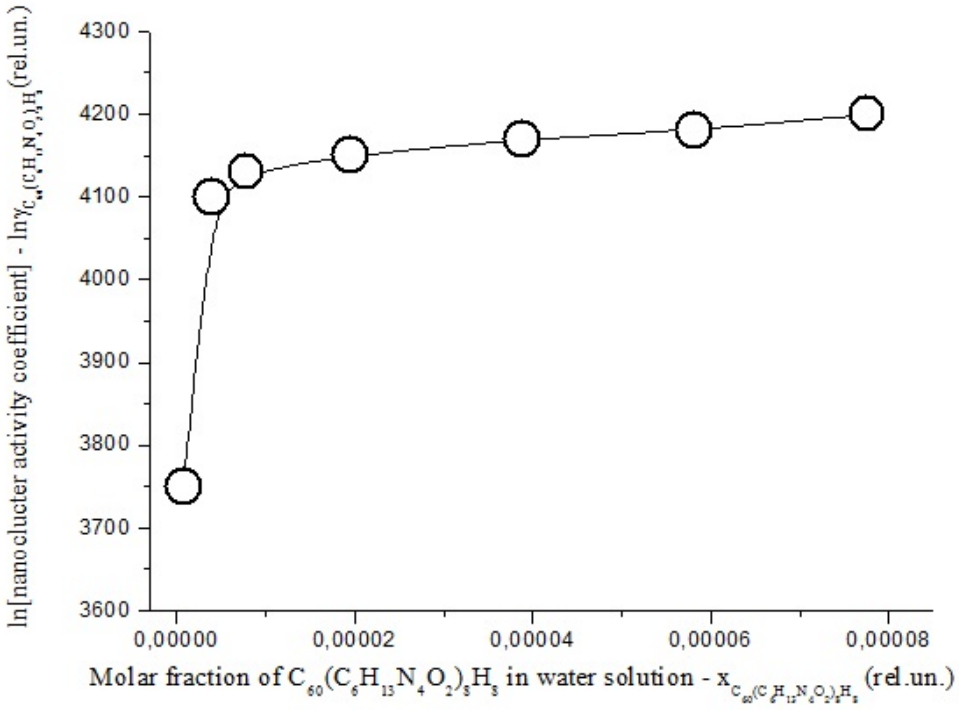


FIG. 7. The dependence of ln of $C_{60}(C_6H_{12}NaN_4O_2)_8H_8$ activity coefficients ($\ln\gamma_{\text{nanocluster}}$) in $C_{60}(C_6H_{12}NaN_4O_2)_8H_8$ – water solutions against the molar fraction of $C_{60}(C_6H_{12}NaN_4O_2)_8H_8$ in aqueous solutions

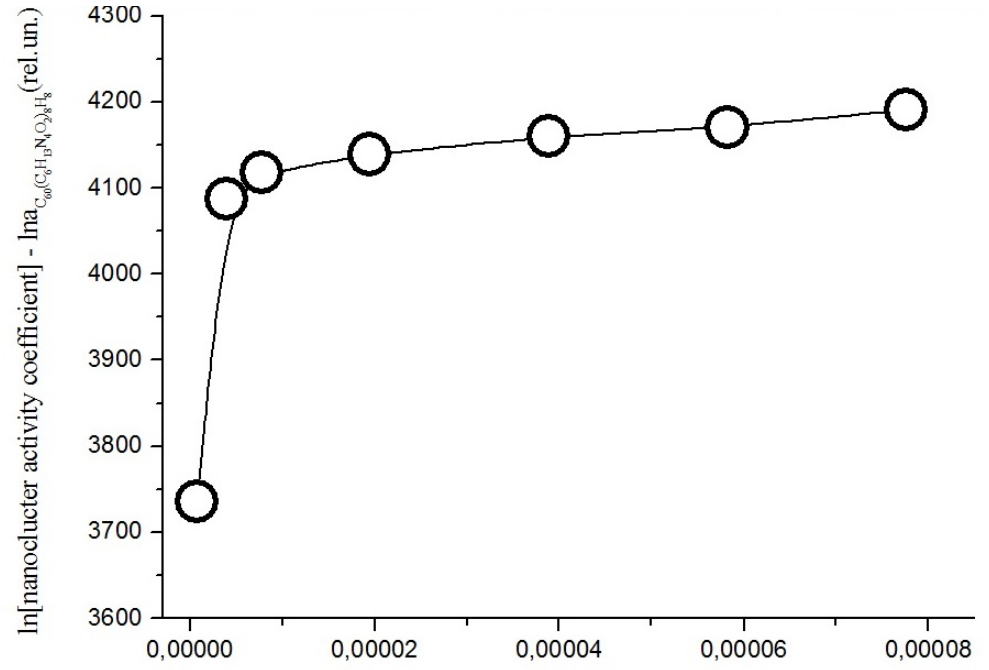


FIG. 8. The dependence of ln of $C_{60}(C_6H_{12}NaN_4O_2)_8H_8$ activity (lnananocluster) in $C_{60}(C_6H_{12}NaN_4O_2)_8H_8$ – water solutions against the molar fraction of $C_{60}(C_6H_{12}NaN_4O_2)_8H_8$ in aqueous solutions

$$G^{\text{mix}} = RT\left[\text{x}_{\text{nanocluster}} \ln a_{\text{nanocluster}} + \text{x}_{\text{H2O}} \ln a_{\text{H2O}}\right]. \tag{9}$$

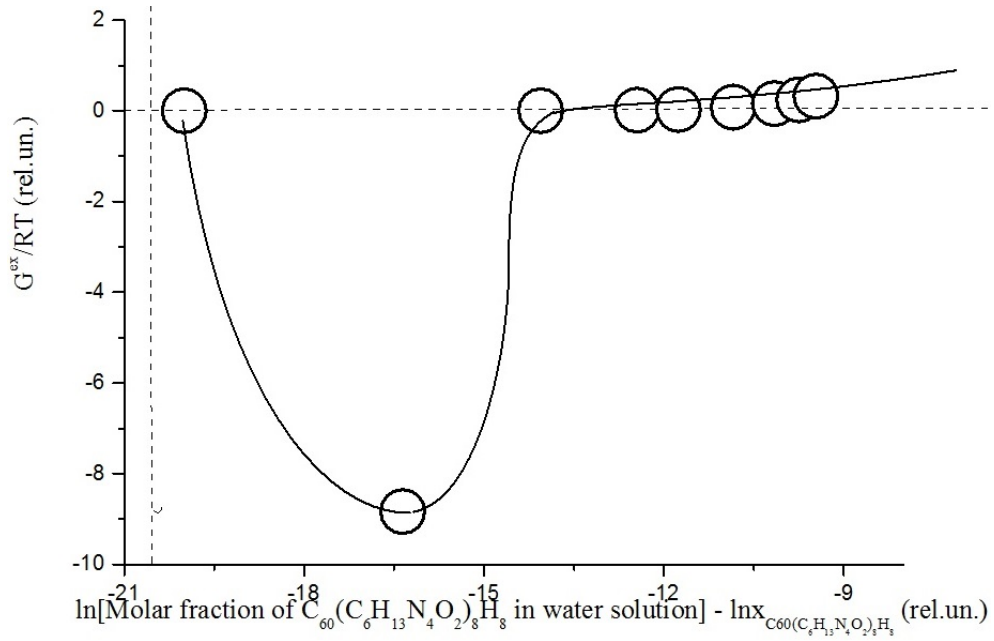


FIG. 9. The dependence of the excess Gibbs energy for solutions ($G^{\text{ex}}$) in $C_{60}(C_6H_{12}NaN_4O_2)_8H_8$ – water solutions against logarithm of molar fraction of $C_{60}(C_6H_{12}NaN_4O_2)_8H_8$ in aqueous solutions

One can see the inflection points in the Figs. 9, 10 where the second derivatives: $\left[\partial^2 G^{\text{mix}}/\partial \text{x}^2_{\text{nanocluster}}\right]_{T,P}$ and $\left[\partial^2 G^{\text{ex}}/\partial \text{x}^2_{\text{nanocluster}}\right]_{T,P}$ change signs or derivatives

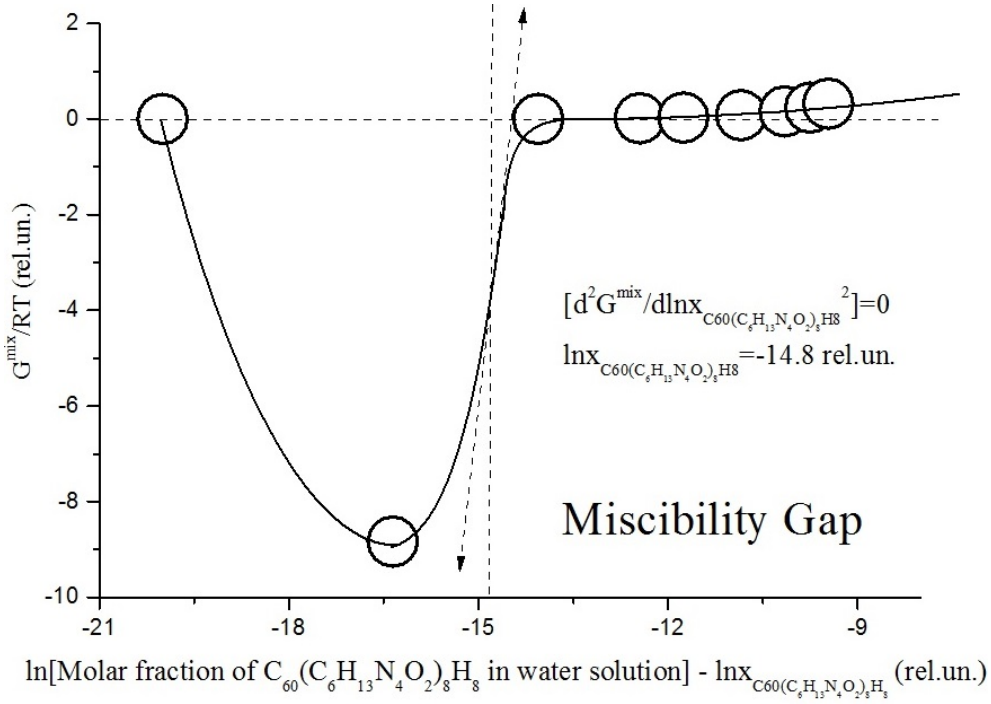


FIG. 10. The dependence of the Gibbs energy mixing for solutions ($G^{\text{mix}}$) and the miscibility gap in $C_{60}(C_6H_{12}NaN_4O_2)_8H_8$ – water solutions against logarithm of molar fraction of $C_{60}(C_6H_{12}NaN_4O_2)_8H_8$ in aqueous solutions

$\left[\partial^2 G^{\text{mix}}/\partial \text{x}^2_{\text{nanocluster}}\right]_{T,P}$ and $[\partial^2 G^{\text{ex}}/\partial \text{x}^2_{\text{nanocluster}}]_{T,P}$ cross through zero. Naturally, this fact takes place together with the crossing through zero of such functions: $\left[\partial^2 G^{\text{mix}}/\partial \ln(\text{x}_{\text{nanocluster}})^2\right]_{T,P}$ and $[\partial^2 G^{\text{ex}}/\partial \ln(\text{x}_{\text{nanocluster}})^2]_{T,P}$. Geometrically, this means that the convexity in the graph $G^e x(\text{x}_{\text{nanocluster}})$ and $G^{\text{mix}}(\text{x}_{\text{nanocluster}})$ is replaced by concavity. And, if the behavior of the first function – $G^{\text{ex}}$ is arbitrarily, the sign of the derivation, $\left[\partial^2 G^{\text{mix}}/\partial \text{x}^2_{\text{nanocluster}}\right]_{T,P}$, over the concentration range of diffusion stability, should be positive. Thus, we can consider that in the region $\text{x}_{\text{nanocluster}} > 4 \cdot 10^{-7}$ rel.un. homogeneous solutions exfoliate and becomes micro-heterogeneous. Light scattering experiments show us that this occurs at the concentration region of the transition from the first type aggregates (the first order clusters of percolation) with the linear dimensions $d_1 \approx 20$ – 80 nm to that of the second type aggregates (the second order clusters of percolation) with the linear dimensions $d_2 \approx 100$ – 400 nm. In other words, there are the concentrations where the system transitions from a nano-heterogeneous one to that of a micro-heterogeneous type.

**Acknowledgements**

Investigations were supported by Russian Found of Basic Research – RFBR (Project No. 15-08-08438) and with the help of the equipment of Resource Center 'Geomodel' (St. Petersburg State University).

**References**

[1] K.N. Semenov, N.A. Charykov, I.V. Murin, Yu.V. Pukharenko. Physico-Chemical Properties of $C_{60}$-tris-malonic-derivative Water Solutions. *J. of Molecular Liquids*, 2015, **202**, P. 50–58.

[2] K.N. Semenov, N.A. Charykov, I.V. Murin, Yu.V. Pukharenko. Physico-chemical properties of the fullerenol-70 water solutions. *J. of Molecular Liquids*, 2015, **202**, P. 1–8.

[3] D.P. Tyurin, K.N. Semenov, et al. Dissociation of Fullerenol-d water solutions and their electric conductivity. *Rus. J. of Phys. Chem.*, 2015, **89** (5), P. 764–768.

[4] I.A. Pestov, V.A. Keskinov, et al. Solubility of $[C_{60}(=C(COOH))_2]_3$ in ternary system $[C_{60}(=C(COOH)_2)_3]$–$SmCl_{3-2}$ at 25 °C. *Rus. J. of Phys. Chem.*, 2015, **89** (6), P. 990–992.

[5] K.N. Semenov, N.A. Charykov, et al. Dependence of the dimension of the associates of water-soluble tris-malonate of light fullerene – $C_{60}[= C(COOH)_2]_3$ in water solutions at 25 °C. *Nanosystems: Physics, Chemistry, Mathematics*, 2015, **6** (2), P. 294–298.

[6] D.P. Tyurin, K.N. Semenov, et al. Dissociation of Fullerenol-70-d in Aqueous Solutions and Their Electric Conductivity. *Russian Journal of Physical Chemistry A*, 2015, **89** (5), P. 771–775.

[7] K.N. Semenov, I.G. Kanterman, et al. Solid–Liquid Phase Equilibria in the Fullerenol-d–$CuCl_2$–$H_2O$ System at 25 °C. *Russian Journal of Physical Chemistry*, 2014, **88** (6), P. 1073–1076.

[8] K.N. Semenov, N.A. Charykov, et al. Synthesis and identification water-soluble tris-malonate of light fullerene – $C_{60}[(=C(COOH)_2]_3$. *Nanosystems: physics, chemistry, mathematics*, 2014, **5** (2), P. 315–319.

[9] K.N. Semenov, N.A. Charykov, et al. Volume properties of water solution and refraction at 25 °C water-soluble tris-malonate of light fullerene- $C_{60}$ $[= C(COOH)_2]_3$. *Nanosystems: physics, chemistry, mathematics*, 2014, **5** (3), P. 427–434.

[10] K.N. Semenov, N.A. Charykov, et al. Poly-thermal solubility and complex thermal analysis of water-soluble tris-malonate of light fullerene – $C_{60}[= C(COOH)_2]_3$. *Nanosystems: physics, chemistry, mathematics*, 2014, **5** (3), P. 435–440.

[11] K.N. Semenov, I.G. Kanterman, et al. Solubility in the Ternary System Fullerenol-d–Uranyl Sulfate–Water at 25 °. *Radiokhimiya*, 2014, **56** (5), P. 493–495.

[12] K.N. Semenov, N.A. Charykov, et al. Concentration dependence of electric conductivity and pH for aqueous solutions of water soluble light fullerene $C_{60}$ $[= C(COOH)_2]_3$ trismalonate. *Nanosystems: physics, chemistry, mathematics*, 2014, **5** (5), P. 709–717.

[13] K.N. Semenov, N.A. Charykov, et al. Fullerenol-d Solubility in Fullerenol-d–Inorganic Salt–Water Ternary Systems at 25 °C. *Industrial & Engineering Chemistry Research*, 2013, **52**, P. 16095–16100.

[14] K.N. Semenov, N.A. Charykov, V.A. Keskinov. Fullerenol Synthesis and Identification. Properties of the Fullerenol Water Solutions. *J. Chem. Eng. Data*, 2011, **56**, P. 230–239.

[15] K.N. Semenov, N.A Charykov. Solubility of light fullerenes and fullerenol in biocompatible with human beings solvents. Chapter in Handbook: *Grapes: Cultivation, Varieties and Nutritional Uses*. Nova Sciences Publishers, Inc., Editor R.P. Murphy et al., 2011, P. 1–48.

[16] K.N. Semenov, N.A. Charykov. Phase Equilibria in the Fullerene Containing Systems. *Handbook on Fullerene: Synthesis, Properties and Applications*, Editor R.F. Verner, C. Benvegny, 2012, P. 1–91.

[17] K.N. Semenov, N.A. Charykov. *Solubility of light fullerenes and it's derivatives*. Germany: Lambert Academic Publishing, 2011, 237 p.

[18] L.B. Gan, C.P. Luo. Water-soluble fullerene derivatives, synthesis and characterization of $\beta$-alanine $C_{60}$ adducts. *Chinese Chemical letters*, 1994, **5** (4), P. 275–278.